CCF Transactions on Networking
https://doi.org/10.1007/s42045-019-00025-7

REGULAR PAPER

Interference-aware lifetime maximization with joint routing and charging in wireless sensor networks

Qi Tan[1] · Yi Qu[1] · Ke Xu[1] · Haiyang Wang[2] · Dan Wang[3] · Meng Shen[4]

Received: 27 March 2019 / Accepted: 11 November 2019

Abstract
Radio Frequency based Wireless power transfer (RF-WPT) has become increasingly popular in recent years. Its ability to harvest Radio Frequency (RF) energy enables a novel approach to charge low-power wireless devices, resulting in benefits to product design, usability, and reliability in wireless sensor networks (WSN). It is however known that RF-WPT also introduces interference to wireless communications, leading to poor data throughput. The joint routing and charging remains a challenging job in RF energy harvesting networks. In this paper, we take initial steps towards understanding both data routing and charger scheduling in WSNs. We propose a smart interference-aware scheduling to maximize network lifetime and avoid potential data loss caused by charging interference. Then, we theoretically prove the optimality of the proposed design, i.e., $1 - \frac{\phi}{W}$, where W is an arbitrary positive integer and ϕ is determined by network properties. The evaluation indicates that the proposed design can guarantee 99% optimality and significantly improve network lifetime in WSNs.

Keywords Wireless power transfer · Energy · Interference · Rechargeable · Sensor networks · Network lifetime

1 Introduction

Radio Frequency based Wireless power transfer (RF-WPT) technology is recognized as a promising way to charge low-power electronics in next generation wireless networks (Liu et al. 2013; Xie et al. 2013). Different from traditional magnetic resonant coupling approaches (Kurs et al. 2007), RF-WPT is a lightweight and more flexible charging technique for low-power RFIDs and sensors (Kellogg et al. 2014; Liu et al. 2013; Xie et al. 2013). This feature gives RF chargers better mobility yet also introduces higher degree of interferences to wireless communications. In particular, the study from Naderi et al. (2014) showed that RF energy transfer would cause data loss and largely reduce wireless throughput. To bring RF-WPT deployments into reality, a smart scheduling approach is therefore required to jointly consider RF charging and wireless data routing.

In this paper, we take initial steps to investigate the potential benefits by jointly optimizing data routing and charger scheduling together. Based on our model analysis, we find that the lifetime maximization problem cannot be solved in polynomial time due to the time dependent constraints. To address this issue, we carefully transform the time dependent continuous problem into a time independent discrete problem. We show that the maximum system lifetime (in

Qi Tan and Yi Qu authors contribute equally to this work.

✉ Ke Xu
xuke@mail.tsinghua.edu.cn

Qi Tan
tanq16@mails.tsinghua.edu.cn

Yi Qu
quy11@mails.tsinghua.edu.cn

Haiyang Wang
haiyang@d.umn.edu

Dan Wang
csdwang@comp.polyu.edu.hk

Meng Shen
shenmeng@bit.edu.cn

[1] Department of Computer Science and Technology, Tsinghua University, Beijing, People's Republic of China

[2] The Department of Computer Science, University of Minnesota at Duluth, Duluth, USA

[3] The Department of Computing, Hong Kong Polytechnic University, Hong Kong, Hong Kong

[4] The Department of Computer Science, Beijing Institute of Technology, Beijing, People's Republic of China

Published online: 29 November 2019

the original problem) can be obtained by solving the time independent discrete problem. To further reduce the complexity of the problem, we relax the energy constraints in the original problem and simplify the charger's travel path to a single TSP (*Traveling Salesman Problem*) path. We then construct a linear programming problem and prove that its optimal solution is an equivalent form of the relaxed problem. Based on this observation, we propose a near-optimal solution to the original problem with theoretically provable optimality $1 - \frac{\phi}{W}$, where W is an arbitrary positive integer and ϕ is determined by system properties such as the maximum charging duration. The contributions of this paper are summarized as follows.

1. To the best of our knowledge, this is the first study that considers RF-WPT charging interference in lifetime maximization of WSNs.
2. Our model analysis successfully approximates the complex joint optimization problem into a linear programming problem.
3. Based on the approximated linear programming, we develop a solution with 99% optimality to the original problem.

The rest of this paper is organized as follows: Sect. 2 presents the system model. After that, the lifetime maximization problem is formulated in Sect. 3. Section 4 explores a near optimal solution with guaranteed performance bound. This solution is then evaluated in Sect. 5. Section 6 further discusses some practical issues in system deployment and Sect. 7 presents related work. Finally, Sect. 8 concludes the paper.

2 Modeling the interference of charging and data routing

We introduce the system model in the following orders to make it easier to understand. Section 2.1 gives the system overview. Section 2.2 describes the basic network model without energy charging. After a mobile charger is introduced, the charger mobility is presented in section 2.3. Then, Sect. 2.4 focuses on charging interference. Section 2.5 describes the data routing under charging interference concerns. Lastly, sensor's energy profiles are illustrated in Sect. 2.6. The related notations are listed in Table 1 for the sake of clarity.

2.1 System overview

As we all know, there are two kinds of wireless charging technologies, non-radiative charging and radiative charging. They are represented by inductive coupling and RF charging, respectively. Inductive coupling requires accurate alignment in charging directions, which is inconvenient. Simultaneously, Kurs et al. (2007) show that the charging efficiency of inductive coupling will be better if charging distance would be eight times the radius of the coils, which may need more changes on sensors. Meanwhile, since RF charging is more appropriate to low-power RFID which means a small node size, it has been put into practice by Peng et al. (2010) and Powercast (2019). In this paper, we use RF charging as our charging method.

We consider a set of wireless sensors N initially equipped with rechargeable batteries and randomly deployed over a two-dimensional area (as the wireless sensors cannot move, their positions are fixed after deployment). Each sensor $i \in N$ generates monitoring data with a rate of g_i, and all sensory data are forwarded to the sink (base station). Whenever sensory data are transmitted or received, sensor i's energy will be consumed.

We define network lifetime T as the duration from the start of monitoring operations to the first time a sensor runs out of energy. To maximize T, a mobile charger is introduced to dynamically charge sensors with low power status. The charger starts from the sink, travels within the network area and visits sensors. In this paper, similar to Guo et al. (2013) and Shi et al. (2011), we assume that a sensor can be charged when the charger visits it. This is based on the fact that charging efficiency drops exponentially with increasing charging distances. As reported in He et al. (2013) and Naderi et al. (2014), when the charger operates with a 3 W ET (*Energy Transmission*) power, sensors located at 1 m away acquire a charging rate of 4 mW. However, this value drops to below 0.01 mW when the distance increases to 10 m.

In fact, there is no exclusive spectrum allocated for power transfer, and most RF-WPT systems operate at the ISM (*Industry, Science and Medical*) band, which is already crowded with communication systems. Although charging interference can be partially alleviated by allocating non-intersect spectrums for power transfer and data routing, it causes severe spectrum efficiency problems. Thus, a smart algorithm that can both maximize network lifetime T and avoid charging interference is urgently required, which is the main objective of this paper.

2.2 Basic network model

Let $g_{ij}(t)$ be the data rate from sensor i to j at time t $(i, j \in N, i \neq j)$. Specifically, $g_{i0}(t)$ represents the data rate from sensor i to the sink. Then, the flow conservation equation at sensor i can be presented as (Shi and Hou 2012):

Table 1 List of notations in the system model

General notations	
N	The set of sensors in the WSN
N_l	The set of interfered sensors during $[t_l, t_l + U(x_l)]$
L	The charger's visit sequence
R	The charging interference radius
d_{il}	Distance between sensor i and sojourn location x_l
x_l	Charger's sojourn location of the lth visit
y_l	Path between two sojourn locations x_l and x_{l+1}
ν_l	The virtual point to represent path segment y_l
W	Number of repeated TSP paths traveled by the charger
Time related notations	
t_l	The time when charger arrives at x_l
$U(x_l)$	Time duration of the charger sojourning x_l
$U(y_l)$	Time duration to traverse y_l
$U(\nu_l)$	Time duration to traverse ν_l and $U(\nu_l) = U(y_l)$
T_0, T_1	End instances of initial and operational intervals
T	Network lifetime (duration of the operational interval)
t_{TL}	Time spent to visit each sensor once during $[0, T_0]$
τ_i	Charging duration for sensor i during $[0, T_0]$
Flow routing related notations	
g_i	Data generation rate of sensor i
$g_{ij}(t)$	Flow routing from sensor i to sensor j at time t
$g_i^s(t)$	Data storing rate for sensor i at time t
$g_i^r(t)$	Data releasing rate for sensor i at time t
$f_{ij}(x_l)$	Flow routing during $[t_l, t_l + U(x_l)]$
$f_{ij}(\nu_l)$	Flow routing during $[t_l + U(x_l), t_{l+1}]$
$f_i^s(x_l)$	Data storing rate for sensor i during $[t_l, t_l + U(x_l)]$
$f_i^r(\nu_l)$	Data releasing rate for sensor i during $[t_l + U(x_l), t_{l+1}]$
g_{max}^r	Maximum data releasing rate
Energy related notations	
E	The total energy assigned for the network
ϖ	The energy charging rate during $[T_0, T_1]$
ϖ_0	The energy charging rate during $[0, T_0]$
h_0	Initial battery of each sensor
e_0	Sensor's energy consumption rate during $[0, T_0]$
H_i	Battery status of sensor i at T_0
e_{il}	Energy consumption of sensor i during $[t_l, t_{l+1}]$
K_{il}	Energy charged for sensor i during $[t_l, t_l + U(x_l)]$
$B_i(t)$	Battery status of sensor i at time t

$$\sum_{k\in N}^{k\neq i} g_{ki}(t) + g_i = \sum_{j\in N}^{j\neq i} g_{ij}(t) + g_{i0}(t) \tag{1}$$

In this paper, we adopt the following energy consumption model (Shi et al. 2011):

$$e_i(t) = \sum_{k\in N}^{k\neq i} \rho g_{ki}(t) + \sum_{j\in N}^{j\neq i} C_{ij} g_{ij}(t) + C_{i0} g_{i0}(t) \tag{2}$$

where $e_i(t)$ is the energy consumption rate for sensor i at time t, ρ is the energy consumption rate for receiving a unit of data rate and C_{ij} is the energy consumption rate for transmitting a unit of data rate from sensor i to sensor j. Specifically, $C_{ij} = \beta_1 + \beta_2 d_{ij}^{\alpha}$, where d_{ij} is the distance between sensor i and j, β_1 and β_2 are coefficients, and α is the path loss index.

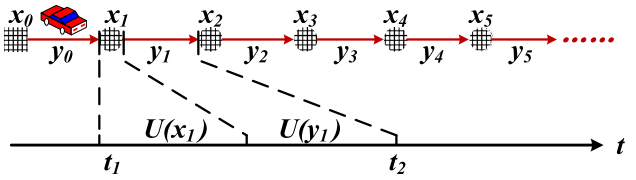

Fig. 1 The charger's travel path consists of sojourn point x_l and path segment y_l. Diamonds and circles represent the location of the sink (x_0) and sensors ($x_1, x_2, ...$). The car represents the mobile charger

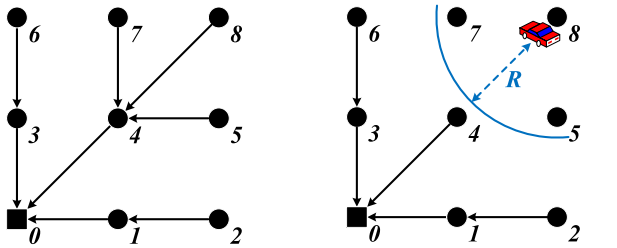

(a) Network topology. **(b)** Charging interference.

Fig. 2 In this example, the network topology is given in (**a**) and a mobile charger sojourns at x_8 to visit sensor 8 in (**b**). Around the charger, sensors 5, 7, 8 are interfered. Solid diamonds and circles represent sink and sensors, respectively

2.3 Charger mobility

As shown in Fig. 1, the charger's travel path is consisted of x_l and y_l ($l \in L$), where L is the sensor sequence that the charger will visit, x_l is a sojourn point and y_l is the path segment between x_l and x_{l+1}. Suppose the charger arrives at x_l at $t = t_l$ and the sojourn duration is $U(x_l)$, then we have $t_{l+1} - t_l = U(x_l) + U(y_l)$, where $U(y_l)$ is the time spent to traverse y_l.

Real experiments in He et al. (2013) and Naderi et al. (2014) have reported that charging rates decrease exponentially with increasing charging distances. For the sake of effective charging, similar to Guo et al. (2013), Shi et al. (2011), we assume that a sensor can be charged only when the charger visits it. Thus, the energy transfer model in He et al. (2013) can be simplified as $K_{il} = \varpi U(x_l)$, where ϖ is the energy transfer rate, K_{il} is the energy charged for sensor i when the charger sojourns at x_l. In particular, $K_{il} > 0$ implies that the charger sojourns at x_l to visit sensor i. Otherwise, $K_{il} = 0$.

2.4 Charging interference

Data routing will be interfered whenever the charger transfers energy. Denote the interference radius as R and the distance between x_l and sensor i as d_{il}. When the charger sojourns at x_l, only if $d_{il} \geq R$, sensor i's data can be transmitted (or received) without loss. Let N_l be the interfered sensor set, then we have $N_l = \{i | i \in N, d_{il} < R\}$. Take Fig. 2 as an example, the charger is visiting sensor 8 and $N_8 = \{5, 7, 8\}$.

As shown in Fig. 1, each charging duration $U(x_l)$ is followed by a travel duration $U(y_l)$. During $U(y_l)$, neither power transfer nor interference exists. We can leverage this regularity to avoid data loss caused by charging interference. Specifically, when data communications are interfered, sensors temporarily store all the to-be-transmitted data. Whenever the interference disappears, the stored data can be released from local storage and transmitted toward the sink. As shown in Fig. 2a, sensors 5, 7 and 8 store data when the charger is charging sensor 8. When the charger finishes charging and moves to the next sensor, all the stored data in sensors 5, 7 and 8 can be forwarded to the sink.

2.5 Data routing

Considering the time interval $[t_l, t_l + U(x_l)]$, the data routing for sensor i can be extended from the basic model as follow:

$$\sum_{k \in N}^{k \neq i} g_{ki}(t) + g_i = \sum_{j \in N}^{j \neq i} g_{ij}(t) + g_{i0}(t) + g_i^s(t)$$

where $g_i^s(t)$ is the data storing rate.

Specifically, for sensor $i \notin N_l$, it is unnecessary to store data, thus the above equation is transformed to the following one:

$$\sum_{k \in N}^{k \neq i} g_{ki}(t) + g_i = \sum_{j \in N}^{j \neq i} g_{ij}(t) + g_{i0}(t), \quad i \notin N_l \tag{3}$$

where $g_i^s(t) = 0$.

As to the interfered sensor $i \in N_l$, data transmission and reception are prohibited to avoid possible loss. Thus we have:

$$g_i = g_i^s(t), \quad i \in N_l \tag{4}$$

where $\sum_{k \in N}^{k \neq i} g_{ki}(t) = 0$, $\sum_{j \in N}^{j \neq i} g_{ij}(t) = 0$ and $g_{i0}(t) = 0$.

During $[t_l, t_l + U(x_l)]$, interfered sensor $i \in N_l$ stores sensory data to its storage. And longer sojourn duration $U(x_l)$ will lead to larger storage occupation. Since a sensor's storage is limited, a maximum sojourn time U_{max} is set to ensure that there is no stored overflow:

$$U(x_l) \leq U_{max}, \quad \forall l \in L \tag{5}$$

When the charger finishes charging at x_l and moves to the next sensor during $[t_l + U(x_l), t_{l+1}]$, no sensor will be interfered. During this interval, for sensor i, we have the following flow conservation equation:

$$\sum_{k\in N}^{k\neq i} g_{ki}(t) + g_i = \sum_{j\in N}^{j\neq i} g_{ij}(t) + g_{i0}(t) - g_i^r(t) \tag{6}$$

where $g_i^r(t)$ is the data releasing rate. To avoid unacceptable delay, data stored during $[t_l, t_l + U(x_l)]$ must be all released out during $[t_l + U(x_l), t_{l+1}]$:

$$\int_{t_l}^{t_l+U(x_l)} g_i^s(t)dt = \int_{t_l+U(x_l)}^{t_{l+1}} g_i^r(t)dt \tag{7}$$

Here, a maximum data releasing rate g_{max} is set to keep interfered sensors in N_l from releasing their stored data with an extremely high transmission rate simultaneously, leading to frequent medium access collisions, i.e.,

$$0 \le g_i^r(t) \le g_{max} \tag{8}$$

Regulating $g_i^r(t)$ will largely decrease the collision possibilities, however, this situation cannot be thoroughly avoided. Then, the remained collisions can be handled by collision resolution protocols such as Yigitel et al. (2011).

2.6 Energy profiles

Studies (Shi et al. 2011; Xie et al. 2013) assumed a scenario that the recharged energy is infinite and the sensor network stays operational forever. In this paper, we focus on a different situation where the total amount of energy assigned for the network is limited to E (Zhu et al. 2010). Specifically, E equals to the sum of sensors' initial and recharged energy. (Since the total amount energy is limited and the time for each charge is confined to less than U_{max}, we have limited the battery capacity to a suitable range.)

Typically, a sensor network's life span is consisted of deployment (before $t = 0$), initial ($[0, T_0]$) and operational intervals ($[T_0, T_1]$). During the deployment interval, sensors are fairly allocated with the same amount of initial battery h_0 and randomly distributed to the interested area. Denote the initial interval as $[0, T_0]$, during which initial operations such as neighbor discovery and routing construction are performed. Meantime, the charger visits each sensor once and charges its battery to an appropriate level to support monitoring operations during the next interval. Denote the charging duration for sensor i as τ_i and the travel time to visit all sensors as t_{TL}, we have:

$$T_0 = t_{TL} + \sum_{i\in N} \tau_i$$

Considering the initial interval, we denote the energy charging rate as ϖ_0. Each sensor consumes energy with a rate of e_0 and sensor i's battery status at $t = T_0$ is H_i. Then, we have:

$$H_i = \varpi_0\tau_i + h_0 - e_0T_0, \quad \forall i \in N$$

Let T_1 be the end time of the sensor network, which is defined as the first time a sensor runs out of energy. During operational interval $[T_0, T_1]$, sensors monitor the interested environment and forward sensory data to the sink. The network lifetime T is defined as the duration of operational interval, i.e., $T = T_1 - T_0$. Because data transmissions are more important than initial interactions, during the operational interval, energy should be transferred more cautiously to avoid large scale interference. Thus we have $\varpi < \varpi_0$, where ϖ and ϖ_0 are energy charging rates during operational and initial intervals, respectively.

Denote e_{il} the energy consumption of sensor i during $[t_l, t_{l+1}]$, we have:

$$e_{il} = \int_{t_l}^{t_{l+1}} e_i(t)dt$$

Let $B_i(t)$ be the battery status of sensor i at time t. To ensure each sensor never runs out of energy before T_1, the following energy constraint must be satisfied:

$$B_i(t_l) = H_i - \sum_{\epsilon=0}^{l}(e_{i\epsilon} - K_{i\epsilon}) \ge 0, \quad i \in N, l \in L \tag{9}$$

Due to the fact that the total energy of the sensor network is limited to E, we have the following constraint:

$$Nh_0 + \varpi_0 \sum_{i\in N} \tau_i + \varpi \sum_{l\in L} U(x_l) \le E \tag{10}$$

where Nh_0, $\varpi_0 \sum_{i\in N} \tau_i$ and $\varpi \sum_{l\in L} U(x_l)$ are total energy ated/recharged during deployment, initial and operational intervals, respectively (Table 2).

Table 2 List of equations (Eqs. (11)–(15) are time discrete equations)

Equations	Description
(1)	Flow routing in the basic network model
(2)	Energy consumption in the basic network model
(3), (11)	Flow routing for un-interfered sensor $i \notin N_l$
(4), (12)	Flow routing for interfered sensor $i \in N_l$
(5)	Regulating the maximum sojourn duration
(6), (13)	Flow routing when the charger is moving
(7), (14)	The stored data must be all released
(8), (15)	Regulating the maximum data releasing rate
(9)	Sensors never run out of energy during $[T_0, T_1]$
(10)	The total energy allocation should be lesser than E

3 Problem formulation

In this section, we first formulate the lifetime maximization problem as a time dependent continuous problem (OR-C). Due to its high complexity, we convert it to a time independent discrete problem (OR-D) and prove that problem (OR-D) achieves the same maximum network lifetime as problem (OR-C). Although problem (OR-D) is also NP-hard, near optimal solutions can be constructed based on it. The description of related equations are listed in Table 2 for the sake of clarity.

3.1 Continuous formulation

Since the charger sojourns and travels within the network area during the whole operational interval, network lifetime T equals to the sum of the charger's sojourn and travel durations during $[T_0, T_1]$ (Guo et al. 2013). Thus, the lifetime maximization problem can be formulated as:

$$\begin{aligned} \max \quad & T = \sum_{l \in L} \left[U(x_l) + U(y_l) \right] \\ \text{s.t.} \quad & \text{Eqs. (3)} - \text{(10)} \end{aligned} \tag{OR-C}$$

In the above formulation, Eqs. (3), (4), (6) are flow conservation constraints. Equation (5) avoids the stored data occupy excessive storage. Equation (7) ensures all stored data are released from sensors' storage. Equation (8) tries to mitigate medium access collisions. Equation (9) ensures that sensors never run out of energy before T_1, and Eq. (10) regulates that the total amount of energy assigned to the network is finite.

Actually, the charger's path planning sub-problem is not modeled in the above formulation. This is based on the finding that near optimal solutions can be constructed without calculating the optimal charger's travel path (see Sect. 4.2). Thus we can omit it in our formulation to keep the system model concise.

Problem (OR-C) is highly complicated and cannot be solved in polynomial time due to the following reasons:

(1) In terms of flow routing, $g_{ij}(t)$, $g_{i0}(t)$, $g_i^s(t)$ and $g_i^r(t)$ are all continuous functions of time t. There may exist infinite number of t, thus infinite number of possible value of data flow functions. Hence, problem (OR-C) is in the form of non-polynomial programming.

(2) The charger's visit sequence L is unknown, which can be determined after a travel path of the charger is found. However, finding the charger's optimal travel path is NP-hard. Considering the simplest path planning problem, TSP, is generally NP-hard.

Before a near optimal solution can be constructed, we convert the time dependent continuous problem (OR-C) to a time independent discrete problem (OR-D), which borrows the idea from (Shi and Hou 2012). Note that the authors only considered the static situation, where the sensor network did not operate when the base station was traveling. This differs from our model in that the sensor network operates continuously during its whole lifetime. Moreover, in our model, network circumstances, sensor and charger behaviors are different from Shi and Hou (2012).

3.2 Discrete formulation

Actually, different relations between $U(x_l)$ and $U(y_l)$ reflect the charger's different behaviors. In particular, there exists three different charger behaviors

- Case 1: $U(x_l) > 0$ and $U(y_l) > 0$. The charger sojourns at x_l for duration $U(x_l)$ and spends $U(y_l)$ to traverse y_l.
- Case 2: $U(x_l) = 0$ and $U(y_l) > 0$. The charger passes x_l without sojourn and spends $U(y_l)$ to traverse y_l.
- Case 3: $U(x_l) = U(y_l) = 0$. The charger directly sets out for location x_{l+1} after x_{l-1} is visited.

An example of different charger behaviors is shown in Fig. 3. To formulate a time independent discrete optimization, we define time independent data flow functions as the average of their time dependent counterparts. As to Case 1, for sensor i during $[t_l, t_l + U(x_l)]$, we have:

$$\text{Sensor } i \text{ to sensor } j\text{:} \quad f_{ij}(x_l) = \frac{\int_{t_l}^{t_l+U(x_l)} g_{ij}(t)dt}{U(x_l)}$$

$$\text{Sensor } i \text{ to the sink:} \quad f_{i0}(x_l) = \frac{\int_{t_l}^{t_l+U(x_l)} g_{i0}(t)dt}{U(x_l)}$$

$$\text{Sensor } i \text{ stores data:} \quad f_i^s(x_l) = \frac{\int_{t_l}^{t_l+U(x_l)} g_i^s(t)dt}{U(x_l)}$$

In the discrete formulation, the time dependent continuous path segment y_l is replaced with the time independent discrete virtual point v_l (see Fig. 4). Let $U(v_l) = U(y_l)$, then data

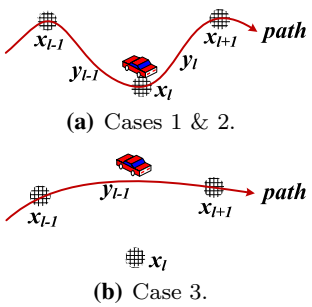

Fig. 3 An illustrative example of different charger behaviors

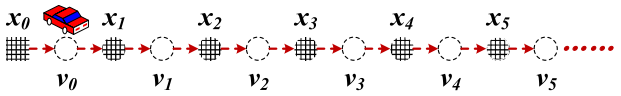

Fig. 4 Replacing the time dependent continuous path segment y_l with time independent discrete virtual point v_l. Then, the charger's travel path is consisted of discrete points x_l and v_l

flow functions during $[t_l + U(x_l), t_{l+1}]$ can be transformed as follows:

$$\text{Sensor } i \text{ to sensor } j\text{:} \quad f_{ij}(v_l) = \frac{\int_{t_l+U(x_l)}^{t_{l+1}} g_{ij}(t)dt}{U(v_l)}$$

$$\text{Sensor } i \text{ to the sink:} \quad f_{i0}(v_l) = \frac{\int_{t_l+U(x_l)}^{t_{l+1}} g_{i0}(t)dt}{U(v_l)}$$

$$\text{Sensor } i \text{ releases data:} \quad f_i^r(v_l) = \frac{\int_{t_l+U(x_l)}^{t_{l+1}} g_i^r(t)dt}{U(v_l)}$$

With regard to Case 2, we define $f_{ij}(x_l) = g_{ij}(t_l)$, $f_{i0}(x_l) = g_{i0}(t_l)$ and $f_i^s(x_l) = g_i^s(t_l)$. Data flow functions during $[t_l + U(x_l), t_{l+1}]$ are transformed similar to Case 1. As to Case 3, we define $f_{ij}(x_l) = g_{ij}(t_l)$, $f_{i0}(x_l) = g_{i0}(t_l)$, $f_i^s(x_l) = g_i^s(t_l)$, $f_{ij}(v_l) = g_{ij}(t_l)$, $f_{i0}(v_l) = g_{i0}(t_l)$ and $f_i^r(v_l) = g_i^r(t_l)$.

In the discrete formulation, for sensor i, when the charger sojourns at x_l and v_l, the flow conservation equations are:

$$\sum_{k\in N}^{k\neq i} f_{ki}(x_l) + g_i = \sum_{j\in N}^{j\neq i} f_{ij}(x_l) + f_{i0}(x_l), \quad i \notin N_l, \tag{11}$$

$$g_i = f_i^s(x_l), \quad i \in N_l \tag{12}$$

and

$$\sum_{k\in N}^{k\neq i} f_{ki}(v_l) + g_i = \sum_{j\in N}^{j\neq i} f_{ij}(v_l) + f_{i0}(v_l) - f_i^r(v_l) \tag{13}$$

For sensor $i \notin N_l$, data communications are not interfered, such that $f_i^s(x_l) = 0$. As to interfered sensor $i \in N_l$, data should be stored to avoid loss. Thus $f_i^s(x_l) = g_i$. As we discussed before, data stored during $[t_l, t_l + U(x_l)]$ should be all released during $[t_l + U(x_l), t_{l+1}]$ to avoid long delay:

$$f_i^s(x_l)U(x_l) = f_i^r(v_l)U(v_l) \tag{14}$$

Similar to the time dependent situation, data releasing rate should be restricted to avoid medium access collisions, i.e.,

$$0 \le f_i^r(v_l) \le g_{max} \tag{15}$$

Energy consumption rates for sensor i during $[t_l, t_l + U(x_l)]$ and $[t_l + U(x_l), t_{l+1}]$ are converted as follows:

$$e_i(x_l) = \sum_{k\in N}^{k\neq i} \rho f_{ki}(x_l) + \sum_{j\in N}^{j\neq i} C_{ij} f_{ij}(x_l) + C_{i0} f_{i0}(x_l)$$

and

$$e_i(v_l) = \sum_{k\in N}^{k\neq i} \rho f_{ki}(v_l) + \sum_{j\in N}^{j\neq i} C_{ij} f_{ij}(v_l) + C_{i0} f_{i0}(v_l)$$

Energy consumed during $[t_l, t_{l+1}]$ is $e_{il} = e_i(x_l)U(x_l) + e_i(v_l)U(v_l)$.

Then, the time independent discrete problem (OR-D) can be formulated as follows:

$$\begin{aligned} \max \quad & T = \sum_{l\in L} [U(x_l) + U(v_l)] \\ \text{s.t.} \quad & \text{Eqs. (5), (9)–(15)} \end{aligned} \tag{OR-D}$$

The following theorem shows that it is feasible to obtain the maximum network lifetime of the original problem (OR-C) by solving problem (OR-D).

Theorem 1 *The optimal solution of problem (OR-D) can achieve the same maximum network lifetime as problem refOR-C).*

We refer the readers to Appendix A for a comprehensive proof.

4 A near optimal solution

This section is organized as follows: Sect. 4.1 discuss the minimum energy routing. Next, we build a linear programming with relaxed energy constraint to approximate the original problem (OR-D). Based on this relaxed problem, a near optimal solution is constructed in Sect. 4.3. Finally, Sect. 4.4 summarizes our solution.

4.1 Minimum energy routing

Peng et al. (2010) show that with enough total-energy and appropriate transfer efficiency, the minimum energy routing would outperform others. As we can meet these conditions, we define the minimum energy routing as the routing scheme.

4.1.1 Basic network model

Naturally, data should be forwarded to the sink in an energy-efficient way, such that the network lifetime can be prolonged. The minimum energy routing in the basic model (Sect. 2.2) can be calculated by the following linear programming:

$$\begin{aligned} \min \quad & \sum_{i\in N} e_i(t) \\ \text{s.t.} \quad & \text{Eqs. (1), (2)} \end{aligned} \tag{MIN-B}$$

We use CPLEX (IBM 2019) to solve problem (MIN-B). Suppose η_i is the resulted energy consumption rate of sensor i, then the minimum total energy consumption rate is $\sum_{i\in N}\eta_i$.

4.1.2 Extended network model

As to the extended network model, the minimum energy routing during $[t_l, t_{l+1}]$ can be calculated by the following optimization:

$$\begin{aligned} \min \quad & \sum_{i\in N} e_{il} \\ \text{s.t.} \quad & \text{Eqs. (11)} - \text{(15)}, \quad U(x_l) = 1 \end{aligned} \tag{MIN-E}$$

Since the duration $[t_l, t_{l+1}]$ is unknown, the charger's sojourn duration $U(x_l)$ is set to a unit of time. Problem (MIN-E) is a quadratic programming due to the quadratic term in $e_i(v_l)U(v_l)$. Before we can solve it, the following theorem is given to convert it to a linear programming.

Theorem 2 *For a given $U(x_l) > 0$, denote g^l_{max} the maximum data generation rate for all interfered sensors, i.e., $g^l_{max} = max(g_i), i \in N_l$. To obtain the minimum energy routing during $[t_l, t_{l+1}]$, equality $U(v_l) = \lambda_l U(x_l)$ must hold, where*

$$\lambda_l = \frac{g^l_{max}}{g_{max}} > 0$$

Note that g_{max} is the maximum data releasing rate. We refer the readers to Appendix B for a comprehensive proof.

Based on the above theorem, problem (MIN-E) can be converted to a linear programming and solved by CPLEX. Suppose the resulted energy consumptions of sensor i during $[t_l, t_l + U(x_l)]$ and $[t_l + U(x_l), t_{l+1}]$ are ε_{il} and μ_{il}, respectively. Then, the minimum total energy consumption during $[t_l, t_{l+1}]$ is $\sum_{i\in N}[\varepsilon_{il}U(x_l) + \mu_{il}U(v_l)]$.

4.1.3 Minimum energy routing and charger behaviors

As we mentioned before, charger behaviors can be reflected by the relation between $U(x_l)$ and $U(v_l)$, which also affects the minimum energy routing. Take Fig. 5 as an example, if $U(x_l) = 0$ and $U(v_l) > 0$, sensors only need to forward newly generated data during $[t_l + U(x_l), t_{l+1}]$. However, if $U(x_l) > 0$ and $U(v_l) > 0$, sensors are required to forward both stored and newly generated data during $[t_l + U(x_l), t_{l+1}]$. Since we cannot predict the values of $U(x_l)$ and $U(v_l)$, each relation should be considered carefully. In particular, four possible relations are listed below:

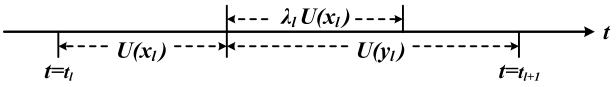

Fig. 5 Relations between $U(x_l)$ and $U(v_l)$

- (1) Relation 1: $U(x_l) > 0$ and $U(v_l) > \lambda_l U(x_l)$
- (2) Relation 2: $U(x_l) > 0$ and $U(v_l) = \lambda_l U(x_l)$
- (3) Relation 3: $U(x_l) = 0$ and $U(v_l) > 0$
- (4) Relation 4: $U(x_l) = 0$ and $U(v_l) = 0$

Based on results obtained from problem (MIN-B) and (MIN-E), we give the following proposition to calculate sensor i's energy consumption during $[t_l, t_{l+1}]$ regardless of the relation between $U(x_l)$ and $U(v_l)$.

Proposition 1 *Suppose the minimum energy routing is always adopted during the operational interval $[T_0, T_1]$. Then the energy consumption of sensor i during $[t_l, t_{l+1}]$ can be calculated by*:

$$e_{il} = \varepsilon_{il}U(x_l) + \mu_{il}\lambda_l U(x_l) + [U(v_l) - \lambda_l U(x_l)]\eta_i$$

We refer the readers to Appendix C for a comprehensive proof.

4.2 Problem relaxation

Actually, charger scheduling is consisted of finding the charger's optimal travel path consisting of x_l and v_l, and deciding durations $U(x_l)$ and $U(v_l)$. To construct a near optimal solution to the original problem (OR-D), we temporarily neglect the maximum sojourn time constraint Eq. (5) and relax the energy constraint Eqs. (9)–(16). Then, a relaxed problem can be built as follows:

$$\max \quad T = \sum_{l\in L}\left[U(x_l) + U(v_l)\right] \tag{RLX}$$

$$\begin{aligned} \text{s.t.} \quad & \text{Eqs. (10)} - \text{(15)} \\ & B_i(T_1) = H_i - \sum_{l\in L}(e_{il} - K_{il}) = 0, \quad \forall i \in N \end{aligned} \tag{16}$$

Since path planning is generally NP-hard, we simplify the charger's travel path to a single TSP path to reduce the complexity of problem (RLX). Further, we suppose the minimum energy routing is adopted during the whole operational interval $[T_0, T_1]$. Then a linear programming can be constructed as follows:

$$\max \quad T = \sum_{l\in L}[U(x_l) + U(v_l)] \tag{LP-T}$$

$$\text{s.t.} \quad \text{Eq. (10)}, \quad L = N \\ U(v_l) \geq \lambda_l U(x_l), \quad \forall l \in L \tag{17}$$

$$\sum_{l \in L} e_{il} - \varpi U(x_i) = H_i, \quad \forall i \in N \tag{18}$$

Note that $L = N$ refers to the fact that the charger's travel path is a single TSP path. Due to the adoption of minimum energy routing, constraint Eq. (16) is equivalently transformed to Eq. (18). Details are omitted to conserve space.

We give the following theorem to show that it is sufficient to solve problem (LP-T) for the objective of lifetime maximization in problem (RLX).

Theorem 3 *The optimal solution of problem (LP-T) is also the optimal solution of problem (RLX).*

We refer the readers to Appendix D for a comprehensive proof.

4.3 Satisfying all constraints

Theorem 3 shows that the optimal solution of problem (RLX) can be obtained by solving linear programming problem (LP-T). However, comparing to the original problem (OR-D), problem (RLX) lacks of two constraints: sojourn time constraint Eq. (5) and energy constraint Eq. (9). In this part, we will show the way to construct a near optimal solution of problem (OR-D) that meets all constraints.

4.3.1 Sojourn time constraint Eq. (5)

To satisfy the sojourn time constraint, we divide the single TSP path into W repeated TSP paths, where W is an arbitrary positive integer. During each TSP path, sojourn time $U(x_l)$ is reduced by $\frac{1}{W}$. Eq. (5) can be satisfied only if W is large enough. We construct the following linear programming:

$$\max \quad T = W \sum_{l \in N} [U(x_l) + U(v_l)] \tag{LP-W}$$

$$\text{s.t.} \quad \text{Eq. (17)}, \quad L = N \\ \sum_{l \in L} e_{il} - \varpi U(x_i) = \frac{H_i}{W}, \quad \forall i \in N \tag{19}$$

$$Nh_0 + \varpi_0 \sum_{i \in N} \tau_i + W\varpi \sum_{l \in L} U(x_l) \leq E \tag{20}$$

We give the following theorem to show that the maximize lifetime T is irrelevant to W.

Theorem 4 *Suppose P^* is the optimal solution of problem (LP-T) with the maximum network lifetime T^*. Then, T^* can be achieved by problem (LP-W) regardless of W.*

We refer the readers to Appendix E for a comprehensive proof.

Similar to Theorem 4, we can prove that if $U(x_l)$ and $U(v_l)$ are optimal results of problem (LP-T), then $\frac{U(x_l)}{W}$ and $\frac{U(v_l)}{W}$ are optimal results of problem (LP-W). The network lifetime T is irrelevant to W, however, the value of W will decide whether the sojourn time constraint is satisfied. Suppose the optimal sojourn time obtained by solving problem (LP-T) is $U^t(x_l)$. Then, the maximum sojourn time in problem (LP-W) must be shorter than U_{max}, i.e.,

$$max\left(\frac{U^t(x_l)}{W}\right) \leq U_{max}$$

Thus we have

$$W \geq \frac{max(U^t(x_l))}{U_{max}}, \quad W \in Z^+$$

When the above inequality holds, the solution to problem (LP-W) satisfies the sojourn time constraint Eq. (5).

4.3.2 Energy constraint Eq. (9)

We focus on one of the W repeated TSP paths. Suppose the optimal solution of problem (LP-W) consists of e^*_{il}, $U^*(x_l)$ and $U^*(v_l)$, and that t^* is the time required to finish one TSP path. Based on Eq. (19), during one TSP path, sensor i's energy consumption comes from two sources: sensor i's initial battery $\frac{H_i}{W}$ and energy replenished by the charger, i.e., $\varpi U^*(x_i)$.

Before the charger visits and recharges sensor i, energy from sensor i's initial battery may be depleted, i.e., $\frac{H_i}{W} \leq \sum_{l \in N} e^*_{il}$. Thus, the energy constraint Eq. (9) is violated. Take the dash line in Fig. 6 as an example, at time t_l, the charger sojourns at x_l and the energy remained in sensor i's battery is $B_i(t_l)$. Before the charger arrives at sensor i when $t = t_i$, its battery depletes and the energy constraint is violated. To avoid it, as the solid line shown in Fig. 6, we only need to assign sensor i with additional energy $\varpi U^*(x_i)$. Suppose each sensor is assigned with an additional energy ζ, we have

$$\zeta = max(\varpi U^*(x_i)), \quad \forall i \in N \tag{21}$$

The total amount of additional energy $N\zeta$ cannot be allocated directly from E since energy allocation is determined after we solve problem (LP-W). However, we can cancel the last $\phi \in Z^+$ TSP paths and assign the reserved energy carried by the charger. The reserved energy should be large enough

to guarantee each sensor is assigned with energy ζ during initial interval, thus we have:

$$\phi\varpi \sum_{i\in N} U^*(x_i) \geq N\zeta\left(1+\frac{Ne_0}{\varpi_0}\right)$$

where the left part is the reversed energy, $N\zeta$ is the total required additional energy, and $N\zeta\frac{Ne_0}{\varpi_0}$ is the energy consumed to assign $N\zeta$. Then, we can obtain:

$$\phi \geq \frac{N\zeta(Ne_0+\varpi_0)}{\varpi\varpi_0\sum_{i\in N}U^*(x_i)}$$

where ϕ is irrelevant to W.

4.4 Solution summary

Now, we give a summary of our near optimal solution:

1. Let $L = N$, for each sojourn location x_l ($l \in N$), calculate N_l^* and λ_l^*.
2. Next, solve problems (MIN-B) and (MIN-E) to obtain the minimum energy routing. For each sensor $i \in N$, calculate η_i^*, ε_{il}^* and μ_{il}^*.
3. Based on η_i^*, ε_{il}^* and μ_{il}^*, solve problem (LP-T). The optimal solution consists of $U^t(x_l)$, $U^t(v_l)$, τ_i^t and $T^t = \sum_{l\in N}[U^t(x_l)+U^t(v_l)]$. Note that T^t is an upper bound of the proposed near optimal solution since it is the optimal solution of the relaxed problem (RLX).
4. Solve problem (LP-W) to obtain the optimal results $U^*(x_l)$ and $U^*(v_l)$. Set $W^* = \lceil\frac{max(U^t(x_l))}{U_{max}}\rceil$, $\zeta^* = max(\varpi U^*(x_i))$ and $\phi^* = \lceil\frac{N\zeta^*(Ne_0+\varpi_0)}{\varpi\varpi_0\sum_{i\in N}U^*(x_i)}\rceil$.
5. Finally, the near optimal solution of the original problem (OR) are constructed as follows: (i) Let $\tau^* = \tau_i^t + \frac{\zeta^*}{\varpi_0}$, during the initial interval, the charger charges each sensor, e.g., i, with energy of $\varpi_0\tau_i^*$. (ii) Adopt the minimum energy routing during the whole network lifetime. Specifically, during $[t_l, t_l+\lambda_l U^*(x_l)]$ and $[t_l+\lambda_l U^*(x_l), t_{l+1}]$, adopt minimum energy routings obtained from problems (MIN-E) and (MIN-B), respectively. (iii) Solve problem (LP-W) and the charger travels $W^*-\phi^*$ repeated TSP paths. Thus, the near optimal network lifetime $T^* = (W^*-\phi^*)\sum_{l\in N}[U^*(x_l)+U^*(v_l)]$.

We summarize our near optimal solution procedure in Table 3. The complexity of our algorithm depends on the complexity of solving linear programming, which is acceptable.

Since T^t is an upper bound of T^*, the optimality of our near optimal solution is:

$$\frac{T^*}{T^t} = \frac{(W^*-\phi^*)\sum_{l\in N}[U^*(x_l)+U^*(v_l)]}{\sum_{l\in N}[U^t(x_l)+U^t(v_l)]} = 1-\frac{\phi^*}{W^*}$$

5 Evaluation

In this part, we first give a numerical example to present some interesting results of our solution. Then, we extensively evaluate it under different parameter settings and reveal insights of the solution performance. Finally, we give some comparisons to show the effectiveness of the proposed solution.

Assuming that sensors are randomly distributed over a $200m * 200m$ two-dimensional square area, the sink is located at (0, 0) and sensors' data generation rate are randomly generated within [1, 10] kb/s. The energy consumption coefficients $\beta_1 = 50$ nJ/b, $\beta_2 = 0.0013$ pJ/$(b \cdot m^4)$, $\alpha = 4$ and $\rho = 50$ nJ/b. The charger sojourns at the sink when $t = 0$.

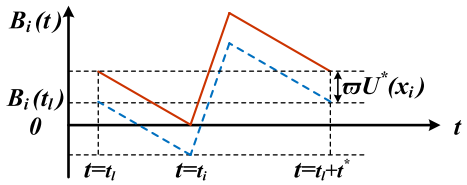

Fig. 6 Satisfying energy constraint Eq. (9) by assigning sensor i with additional energy $\varpi U^*(x_i)$

Table 3 A summary of the proposed solution procedure

Solution procedure
1. Let $L = N$, for each sojourn location x_l ($l \in N$), calculate N_l^* and λ_l^*
2. Solve problems (MIN-B) and (MIN-E) by CPLEX, calculate η_i^*, ε_{il}^* and μ_{il}^*
3. Solve problem (LP-T) by CPLEX, calculate $U^t(x_l)$, $U^t(v_l)$, τ_i^t
4. Set $W^* = \lceil\frac{max(U^t(x_l))}{U_{max}}\rceil$
5. Solve problem (LP-W) by CPLEX, calculate the optimal results $U^*(x_l)$ and $U^*(v_l)$
6. Set $\zeta^* = max(\varpi U^*(x_i))$; $\phi^* = \lceil\frac{N\zeta^*(Ne_0+\varpi_0)}{\varpi\varpi_0\sum_{i\in N}U^*(x_i)}\rceil$ and the initial energy allocation $E_{initial} = \phi^*\sum_{l\in N}[U^*(x_l)+U^*(v_l)$
7. Obtain $T^* = (W^*-\phi^*)\sum_{l\in N}[U^*(x_l)+U^*(v_l)]$

The energy charging rates during initial and operational intervals are $\varpi_0 = 1$ J/s and $\varpi = 0.05$ J/s, respectively. The charging interference radius is $R = 50$ m.

The total energy E is proportional to the number of sensors, i.e., $E = N \times 10^4$ J. The beginning battery is set to $h_0 = 1000$ J and the energy consumption rate during initial interval is $e_0 = 1 \times 10^{-3}$ J/s. Moreover, the maximum sojourn time is $U_{max} = 60$ s, the maximum data releasing rate is $g_{max} = 10$ kb/s, and the charger's travel time during initial interval is $t_{TL} = 1000$ s.

5.1 A numerical example

Here, a 15-sensor random network with initial energy $h_0 = 100$ J is built and h_0 is set to a small value to accommodate the small network. Following default settings, we run the solution and obtain the optimal network lifetime $T = 9.4 \times 10^6$ s. Details are listed in Table 4, where (*x-axis*, *y-axis*) represents sensor locations. Based on Step (4) of our solution, $W = 7580$ and $\phi = 4$. Thus the network terminates after the charger repeats $W - \phi = 7576$ TSP paths. In this case, the optimality of our near optimal solution is $1 - \frac{\phi}{W} = 99.95\%$.

5.2 Parameter analysis

We increase the number of sensors to 50 and analyze how the parameter settings influence our solution. Four parameters are considered here: energy charging rate ϖ, interference radius R, energy consumption rate during initial interval e_0, and the maximum data releasing rate g_{max}. For each parameter, we consider the following solution details: network lifetime T, energy allocated during initial/operational intervals, solution optimality, and the number of repeated TSP paths.

We vary *varpi* from 0.01 J/s to 0.1 J/s while keeping other parameters unchanged. From Fig. 7a, we find that ϖ has limited influence to T. However, it affects the constituent parts of T: sojourn and travel time. With larger ϖ, the charger spends less time on energy transfer (sojourn), but more time on traveling. Impressively, as shown in Fig. 7b, the near optimal solution always achieves above 99% optimality. The high optimality means through our scheduling, we can nearly reach the upper limit of lifetime, under the condition of limited energy, in ideal surroundings (Once the environment and conditions change, such as taking

Table 4 A numerical example: solution details

Variables	Sensor index (i)														
	1	2	3	4	5	6	7	8	9	10	11	12	13	14	15
x-axis	91	171	63	14	37	131	92	118	100	177	11	32	177	34	194
y-axis	80	186	86	40	146	159	22	165	23	70	66	179	115	107	95
g_i	5	2	6	3	3	6	4	3	7	8	4	4	1	8	2
λ_i	0.60	0.60	0.80	0.40	0.80	0.60	0.70	0.60	0.70	0.80	0.80	0.40	0.80	0.80	0.80
τ_i	3	3	3	2.32E4	3	3	3	3	3	3	2.04E4	3	3	7.22E3	3
H_i	951	951	951	2.41E4	951	951	951	951	951	951	2.14E4	951	951	8.17E3	951
$U(x_i)$	44.7	0.68	23.6	0	8.86	17.1	60	19.5	31.2	40.5	0	5.87	1.17	0	0.59
$U(v_i)$	839	0.41	18.9	0	7.09	10.2	42	11.7	21.9	32.4	0	2.34	0.93	0	0.47

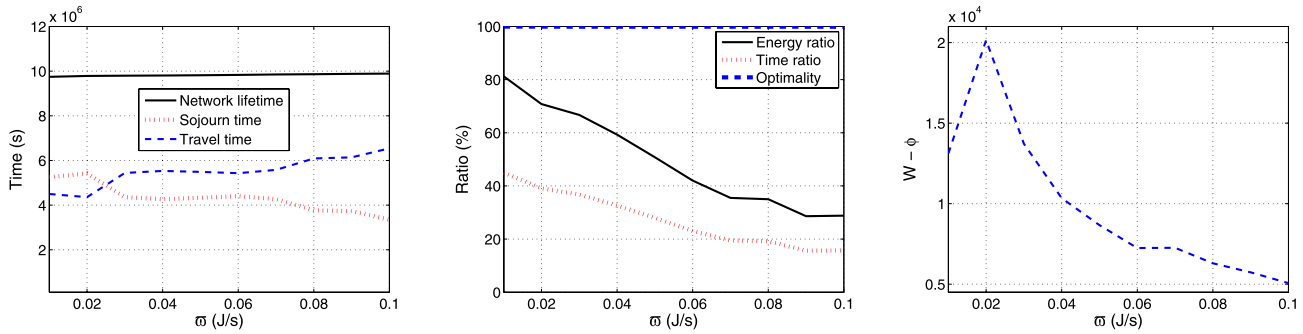

(a) Network lifetime details.

(b) Allocation ratio during T_0 and optimality.

(c) Number of repeated TSP paths.

Fig. 7 Parameter analysis of charging rate ϖ

energy dissipation into consideration, we may not reach such a good result).

We can find that ϖ has direct influences on energy allocation. Since the initial battery h_0 is constant, we focus on energy allocation ratio during the initial interval, i.e., $\frac{\sum_{i\in N}\varpi_0\tau_i}{E}$. In Fig. 7b, when $\varpi = 0.01$ J/s, 81.2% of energy is allocated during $[0, T_0]$ while less than 10% energy is allocated during $[T_0, T_1]$. When ϖ increases to 0.1 J/s, above 60% energy is allocated during $[T_0, T_1]$ while only 28.8% is during $[0, T_0]$. The ratio $\frac{T_0}{T}$ follows the same trend.

Another factor we consider is the number of TSP paths, i.e., $W - \phi$. As shown in Fig. 7c, as ϖ increases, $W - \phi$ increases at first and after a threshold ($\varpi = 0.02$ J/s) is surpassed, $W - \phi$ decreases quickly. The incremental part is caused by the charger's frequent movement to transfer more energy. After $\varpi \geq 0.02$, the charger has stronger charging ability and it could sojourn longer to achieve higher energy transfer. Thus, $W - \phi$ decreases.

As to interference radius R, the network lifetime varies slowly (see Fig. 8a). Compared to ϖ, an apparent characteristic of R is the large randomness. Although T keeps stable, sojourn and travel durations vary widely. With the increase of R, generally, the sojourn time decreases while the travel time increases. Since larger R causes more interfered sensors, chargers tend to sojourn less when R is large. The energy and time ratios both increase as R increases, also with random fluctuations (see Fig. 8b). In Fig. 8c, the large randomness of $W - \phi$ is mainly caused by sensor distribution. For example, when the charger is visiting sensor i with $R = 20$ m, 3 sensors around i may be interfered. However, this number may increase to 15 when $R = 40$ m due to the random distribution of sensors.

The initial energy consumption rate e_0 has significant effect on network lifetime. As shown in Fig. 9a, when e_0 increases, network lifetime decreases quickly. Specifically, when e_0 is small ($e_0 < 1.2 \times 10^{-3}$ J/s), sojourn time increases while travel time decreases with the increase of e_0. The reason is apparent: larger e_0 leads to more energy consumption during the initial interval. Thus, T_0 is kept small and more energy is allocated during the operational interval, leading to longer sojourn time. After $e_0 > 1.2 \times 10^{-3}$ J/s, as the increase of e_0, the sojourn and travel time in Fig. 9a decrease

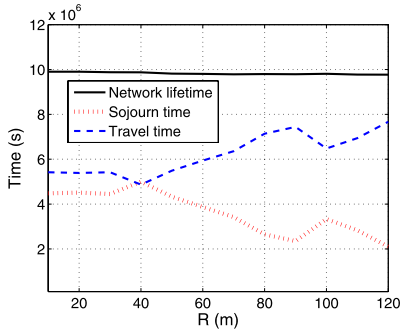

(a) Network lifetime details.

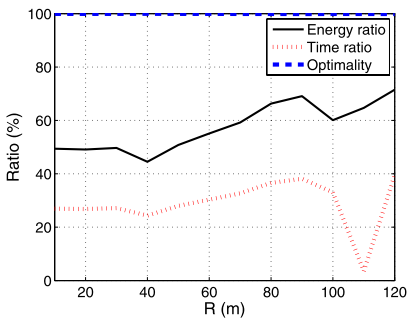

(b) Allocation ratio during T_0 and optimality.

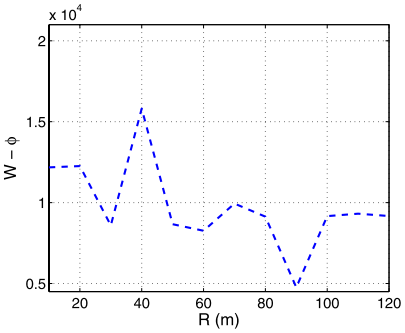

(c) Number of repeated TSP paths.

Fig. 8 Parameter analysis of interference radius R

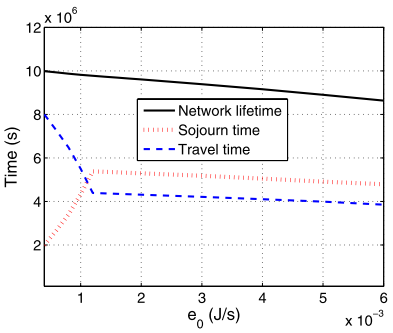

(a) Network lifetime details.

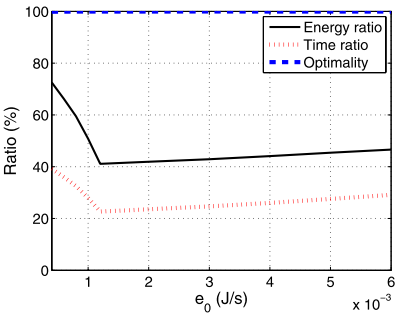

(b) Allocation ratio during T_0 and optimality.

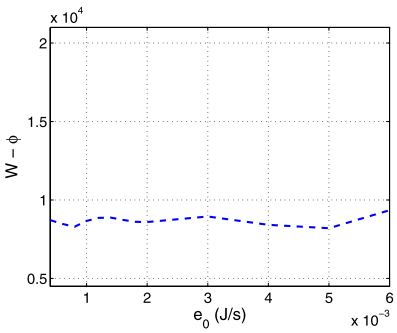

(c) Number of repeated TSP paths.

Fig. 9 Parameter analysis of the initial energy consumption rate e_0

while energy and time ratio in Fig. 9b increase, all in a linear manner. The decreased sojourn/travel times are caused by reduced network lifetime.

The reasons of increased energy/time ratios are more complex. To obtain longer network lifetime, the sensors must be allocated with sufficient energy. Moreover, energy should be allocated among sensors in a balanced way. When e_0 surpasses a threshold ($e_0 > 1.2 \times 10^{-3}$ J/s), the energy balance becomes much more important than the energy quantity. Although larger e_0 leads to more energy consumption during the initial interval, longer initial duration is still required to make energy allocation balanced. As to $W - \phi$ in Fig. 9c, e_0 shows insignificant importance.

At last, we analyze the maximum data releasing rate g_{max}. As g_{max} increases, network lifetime and sojourn time increase while travel time decreases as shown in Fig. 10a. When $g_{max} \in [1, 6]$ kb/s, sojourn and travel times vary quickly. While after $g_{max} > 6$ kb/s, both vary slowly. Energy and time ratios in Fig. 10b present similar regularities. The same as e_0, g_{max} shows trivial importance to $W - \phi$.

5.3 Performance comparison

We set up two baselines to compare with our near optimal solution. The first one is the minimum energy routing, which is pervasively adopted in practice. In this case, the total energy E is averagely allocated among sensors. After deployment, sensors forward sensory data to the sink with a minimum energy routing. The second algorithm is named as perfect allocation. Suppose the minimum energy routing is adopted by the sensor network, the total energy E is allocated based on the sensor energy consumption in a perfect way, which means that sensor batteries will be depleted simultaneously when the network terminates. We note that perfect allocation is unreachable in practice since we cannot obtain sensor energy consumption information before the energy is actually consumed. Perfect allocation represents the possible maximum network lifetime while the minimum energy routing stands for the generally adopted solution.

To evaluate our solution in different network sizes, the number of sensors is varied from 40 to 100. Impressively, as shown in Fig. 11, with the same amount of the total energy E, the network lifetime of our solution is 7.15–22.75 times longer than that of the minimum energy routing which is pervasively adopted. Moreover, the ratio between our solution and the perfect allocation varies from 92.8% to 97%, which validates the high effectiveness. In terms of energy efficiency, as shown in Fig. 12, less than 0.2% energy is wasted by our solution. Compared to perfect allocation, which utilizes 100% energy, our solution presents high efficiency. The minimum energy routing wastes above 86% energy. This is because the network lifetime is determined by the sensor with the largest energy consumption. When the network terminates, a large part of energy is remained in the batteries of light-burdened sensors.

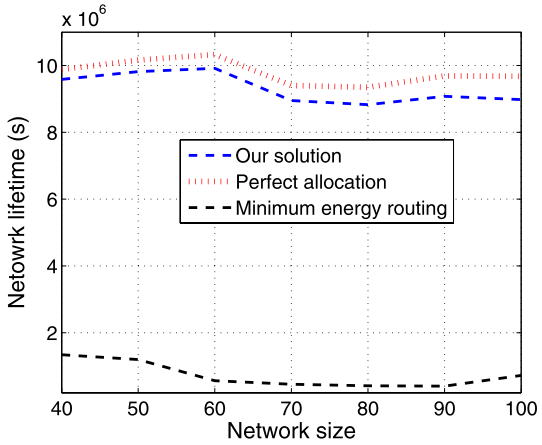

Fig. 11 Performance comparison: network lifetime

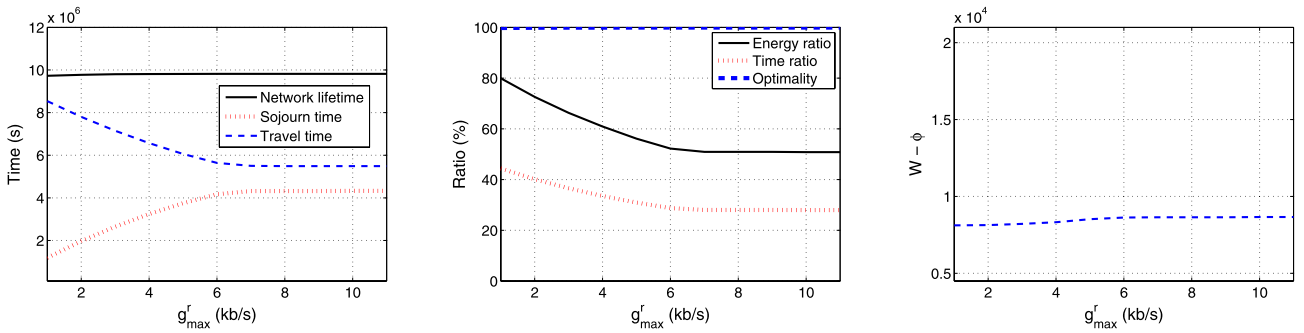

(a) Network lifetime details. **(b)** Allocation ratio during T_0 and optimality. **(c)** Number of repeated TSP paths.

Fig. 10 Parameter analysis of the maximum data releasing rate g_{max}

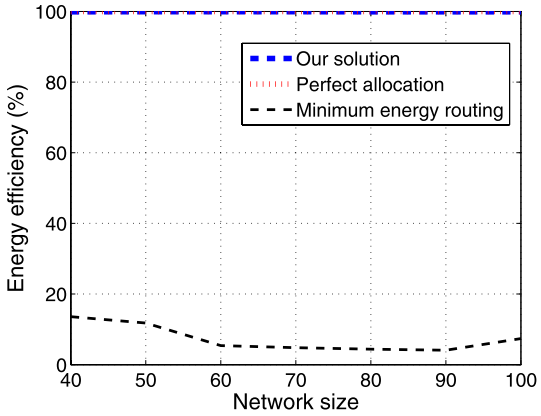

Fig. 12 Performance comparison: energy efficiency

6 Further discussion

RF-WPT is known to be a promising way to solve energy bottlenecks for low power devices. Our study has provided evidences that RF-WPT chargers can be utilized to promote sensor network performance at the cost of introducing higher degree of interferences. Since deploying mobile relays (Park and Heidemann 2011; Somasundara et al. 2006; Qu et al. 2015) in wireless sensor networks are mature technologies with years of exploration, implementing the proposed solution will not pose severer challenges. A simple and practical design is to make the charger a coordinator that controls sensor-charger collaboration (Anastasi et al. 2007; Li et al. 2013).

Our work remains an initial attempt toward jointly considering communication and charger scheduling in interference-aware environments. There are still many open issues that can be further explored, and we hereby list three in which we are particularly interested.

Sensor-charger interaction overheads In our investigation, communications among sensors are optimized. However, in real environments, interactions between the charger and sensors are inevitable and lead to communication overheads. Efficient designs that minimize communication overheads are to be developed.

Sensor storage and charger travel distance Except for energy, storage is also quite limited in sensors. To avoid large storage usage, in our solution, the charger sojourn time is restricted. This may cause frequent charger movements, leading to longer travel distance. Therefore, trade-offs between sensor storages and charger travel distances are worth of further explorations.

Power transfer efficiency In this study, we focus on allocating constant total energy E among sensors. To achieve this goal, in practice, more energy than E will be transferred by the charger due to efficiency problems. Although there has been researches aiming at promoting power transfer efficiency (Lee and Lorenz 2011; Chen et al. 2013), more researches are still required.

7 Related work

Typically, an RF-WPT system consists of an energy transmitter that radiates RF signals and an energy harvester that collects and converts signal power to appropriate direct currents. In the modern society, probably the most well-known commercial application of RF-WPT is RFID, where the RFID tags collect energy from interrogating radio waves and communicate exclusively with RFID readers. By harvesting energy from ambient RF signals, (Liu et al. 2013) extended the traditional RFID tag with incomplete functions to a mini-computer with full computation, communication and control abilities. Compared to magnetic resonant coupling approaches proposed by Kurs et al. (2007), RF-WPT is recognized as a suitable way to charge devices with ultra-low power requirements such as sensors and RFIDs (Kellogg et al. 2014; Liu et al. 2013; Xie et al. 2013). This is due to the simplicity of RF-WPT that neither large coils (with diameter of 0.6m in Kurs et al. (2007) nor scrupulous resonance alignment is needed. Most importantly, RF-WPT brings about the minimal cost increase, because it can be implemented by adding several basic electronic elements such as rectifier, capacitors and diodes to the existing circuits (Kellogg et al. 2014).

However, RF signals emitted for power transfer always exhibit higher signal strength than low-power data communications. Without special treatments, data transmissions will be heavily interfered after an RF-WPT charger is introduced in WSNs. For example, through experimental studies, Naderi et al. (2014) showed that the RF energy transfer would cause data loss and largely reduce the wireless throughput. The study in Naderi et al. (2014) reported that sensors would experience 100% data loss when the charger was operating within 140 m with 1 W ET(energy transmission) power.

Academic researches have taken important steps towards applying WPT technologies in WSNs (Shi et al. 2011; Xie et al. 2013; Guo et al. 2013; He et al. 2013; Fu et al. 2013; Dai et al. 2014; Zhang et al. 2015). In Shi et al. (2011), a mobile wireless charging vehicle (WCV) is introduced and sensor batteries are replenished in a periodical manner. Adopted in small-scale networks, WCV ensured sensors stay operational forever. The mathematical study in Xie et al. (2013) proved that bundling the base station on the WCV could further promote network performance. Aiming at the maximum network utility, an anchor-point based mobile

data gathering scheme is proposed in Guo et al. (2013), which achieves finer scalability and can be adopted in larger networks. Different from mobile charger approaches, (He et al. 2013) considered the charger deployment problem in static scenarios, which also ensured enough power transfer for sensor networks. Moreover, Fu et al. (2013) studied the minimum charging delay problem while (Dai et al. 2014) attempted to transfer the maximum power under a predefined electromagnetic radiation threshold. Zhang et al. (2015) jointly considered the charger placement and power allocation, aiming at improving energy charging quality. The recent studies mainly focus on sensor-charger cooperation. However, how to avoid charging interference has seldom been examined. This paper takes initial steps to make up the research gap in this area.

8 Conclusion and future work

In this paper, we investigated the joint optimization of maximizing network lifetime and avoiding data loss under charging interference concerns. Considering the complexity of the original problem, we relaxed it and constructed a series of simpler optimizations. Based on them, a near optimal solution with provable $1-\frac{\phi}{W}$ performance guarantee has been developed. The effectiveness of our solution is validated with extensive evaluations and comparisons. In our future work, we will further explore the situation with extremely large scale networks and multiple mobile chargers.

Acknowledgements This work was in part supported by the National Key R&D Program of China with No. 2018YFB0803405, China National Funds for Distinguished Young Scientists with No. 61825204 and Beijing Outstanding Young Scientist Project.

Prove of Theorem 1

Proof Suppose P is the optimal solution of problem (OR-C), which consists of the maximum network lifetime T, the optimal charger's travel path, sojourn/travel durations $U(x_l)$ and $U(y_l)$, data flow functions $g_{ij}(t)$, $g_{i0}(t)$, $g_i^s(t)$ and $g_i^r(t)$. Based on solution P, we can construct a solution P^* with lifetime T^* as follows. First, we keep the charger's travel path and sojourn/travel durations the same as solution P. Then we show that both of these solutions achieve the same network lifetime:

$$T^* = \sum_{l\in L}[U(x_l)+U(v_l)] = \sum_{l\in L}[U(x_l)+U(y_l)] = T$$

Next, we construct data flow functions of solution P^* as described in Sect. 3.2. And we need to show that P^* is a feasible solution of problem (OR-D). Specifically, we need to prove that solution P^* meets constraints Eqs. (5), (9)–(15). Here, we focus on constraint Eq. (13) while others are similar and thus omitted to conserve space. The proofs are based on 3 different cases described in Sect. 3.2.

Considering Case 1, for sensor i, we have:

$$\begin{aligned}
&\sum_{k\in N}^{k\neq i} f_{ki}(v_l) + g_i \\
&= \sum_{k\in N}^{k\neq i} \frac{\int_{t_l+U(x_l)}^{t_{l+1}} g_{ki}(t)dt}{U(v_l)} + \frac{\int_{t_l+U(x_l)}^{t_{l+1}} g_i dt}{U(v_l)} \\
&= \frac{\int_{t_l+U(x_l)}^{t_{l+1}} [\sum_{k\in N}^{k\neq i} g_{ki}(t) + g_i]dt}{U(v_l)} \\
&= \frac{\int_{t_l+U(x_l)}^{t_{l+1}} [\sum_{j\in N}^{j\neq i} g_{ij}(t) + g_{i0}(t) - g_i^r(t)]dt}{U(v_l)} \\
&= \sum_{j\in N}^{j\neq i} f_{ij}(v_l) + f_{i0}(v_l) - f_i^r(v_l)
\end{aligned}$$

Cases 2 and 3 can be proved in the same way. Since all the constraints of problem (*OR-D*) are satisfied by solution P^*, P^* is a feasible solution to problem (*OR-D*).

Finally, we need to show that P^* is the optimal solution of problem (*OR-D*). Suppose $\overline{P}$ is the optimal solution of problem (*OR-D*) with the maximum network lifetime $\overline{T} > T$. Based on $\overline{P}$, we can construct a solution of problem (*OR-C*) with lifetime $\overline{T}$, which contradicts with the fact that T is the maximum network lifetime.

Since we have proved that $T^* = T$, the optimal solution of problem (*OR-D*) can achieve the same maximum network lifetime as problem (*OR-C*), which concludes the proof. □

Proof of Theorem 2

The proof of Theorem 2 is based on the following lemmas.

Lemma 1 *For a given feasible charger travel path and a sojourn point x_l, we have $U(v_l) \geq \lambda_l U(x_l)$.*

Proof Since both g_{max}^l and g_{max} are positive parameters, $\lambda_l > 0$ holds. If $U(x_l) = 0$, $U(v_l) \geq \lambda_l U(x_l) = 0$ holds. Here, we emphasize on proving the $U(x_l) > 0$ case. Based on Eqs. (12), (14) and (15), we can derive:

$$g_i U(x_l) = f_i^s(x_l)U(x_l) = f_i^r(v_l)U(v_l) \leq g_{max}U(v_l) \tag{22}$$

Hence, $g_{max}U(v_l) \geq g_i U(x_l)$ holds for all sensor $i \in N_l$. It holds for the sensor with the maximum data generation rate in N_l, thus $g_{max}U(v_l) \geq g_{max}^l U(x_l)$, which concludes the

proof. Note that this lemma also holds for the time dependent continuous formulation, we omit the proof to conserve space. □

Lemma 2 *Considering a data routing with full sensor participation, denote π_i the minimum energy consumption rate required to forward a unit of data from sensor i to the sink, and the corresponding routing path is F_i. Suppose each sensor has a unit of data generation rate, then, the combination of $\sum_{i\in N} F_i$ is the minimum energy routing with the minimum total energy consumption rate $\sum_{i\in N}\pi_i$.*

Proof It is apparent that $\sum_{i\in N} F_i$ is a routing scheme of the sensor network. Next, we prove $\sum_{i\in N} F_i$ is the minimum energy routing using contradictions. Suppose M^* is a routing scheme that consumes less energy than $\sum_{i\in N}\pi_i$. Thus at least one routing path F_i^* in M^* consumes less energy than π_i, which contradicts with the fact that F_i is the minimum energy routing path. □

Now, we begin to prove Theorem 2.

Proof During $[t_l + U(x_l), t_{l+1}]$, the sensory data generated by sensor i is consisted of two parts: $g_i^s(x_l)U(x_l)$ and $g_iU(\nu_l)$. The former is generated and stored during $[t_l, t_l + U(x_l)]$, and the latter is newly generated during $[t_l + U(x_l), t_{l+1}]$. Suppose the minimum energy routing is adopted during $[t_l, t_{l+1}]$, based on Lemma 2, the total energy consumption is:

$$\begin{aligned}
&\sum_{i\in N}\pi_i[g_i^s(x_l)U(x_l) + g_iU(\nu_l)]\\
&= \sum_{i\in N}\pi_i g_i^s(x_l)U(x_l) + \sum_{i\in N}\pi_i g_iU(\nu_l)\\
&= \sum_{i\in N_l}\pi_i g_iU(x_l) + \sum_{i\in N}\pi_i g_iU(\nu_l)\\
&\geq \sum_{i\in N_l}\pi_i g_iU(x_l) + \sum_{i\in N}\pi_i g_i\lambda_lU(x_l)
\end{aligned}$$

When $U(\nu_l) = \lambda_lU(x_l)$, the total energy consumption during $[t_l + U(x_l), t_{l+1}]$ is minimized, which concludes the proof. □

Proof of Proposition 1

Proof The proofs of Relations 2 and 3 are apparent. After we solve problem (MIN-E), $e_{il} = \varepsilon_{il}U(x_l) + \mu_{il}U(\nu_l)$ can be easily obtained. Here, we focus on Relation 1. We assume that the minimum energy routing during $[t_l, t_{l+1}]$ is unique (the proof of non-unique situation is similar). To prove the proposition, we only need to prove that the total energy consumption $\sum_{i\in N} e_{il}$ is minimal.

Based on Lemma 2, we can derive $\sum_{i\in N}\eta_i = \sum_{i\in N}\pi_i g_i$ and

$$\sum_{i\in N}\mu_{il}\lambda_lU(x_l) = \sum_{i\in N_l}\pi_i g_iU(x_l) + \sum_{i\in N}\pi_i g_i\lambda_lU(x_l) \tag{23}$$

Then, we have:

$$\begin{aligned}
&\sum_{i\in N} e_{il}\\
&= \sum_{i\in N}\varepsilon_{il}U(x_l) + \sum_{i\in N}\mu_{il}\lambda_lU(x_l) + \sum_{i\in N}[U(\nu_l) - \lambda_lU(x_l)]\eta_i\\
&= \sum_{i\in N}\varepsilon_{il}U(x_l) + \sum_{i\in N_l}\pi_i g_iU(x_l) + \sum_{i\in N}\pi_i g_i\lambda_lU(x_l)\\
&\quad + \sum_{i\in N}[U(\nu_l) - \lambda_lU(x_l)]\pi_i g_i\\
&= \sum_{i\in N}\varepsilon_{il}U(x_l) + \sum_{i\in N_l}\pi_i g_iU(x_l) + \sum_{i\in N}\pi_i g_iU(\nu_l)
\end{aligned} \tag{24}$$

where $\sum_{i\in N}\varepsilon_{il}U(x_l)$ is the minimum energy consumption during $[t_l, t_l + U(x_l)]$ and the successive two polynomials together represent the minimum energy routing during $[t_l + U(x_l), t_{l+1}]$, which concludes the proof. □

Proof of theorem 3

The proof is based on the following lemmas.

Lemma 3 *A feasible solution of problem (LP-T) is also a feasible solution of problem (RLX).*

Proof Suppose P is a feasible solution of problem (LP-T) that consists of $U(x_l)$ and $U(\nu_l)$. Since energy consumption results η_i, ε_{il} and μ_{il} are all obtained by solving problems (MIN-B) and (MIN-E), and data routing constraints Eqs. (11)–(15) are naturally satisfied by P. Let the charger travel a single TSP path (with each sensor visited once) and constraint Eq. (18) is equivalent to constraint Eq. (16). Therefore, constraints Eqs. (10)–(16) are all satisfied by solution P. Thus P is a feasible solution to problem (RLX), which concludes the proof. □

Lemma 4 *In terms of problem (RLX), as long as the total sojourn durations $\sum_{l\in N}U(x_l)$ and $\sum_{l\in N}U(\nu_l)$ at each sensor's location remains the same, the network lifetime will remain unchanged regardless of the charger's travel path.*

Proof Since the energy constraint Eq. (9) is relaxed to Eq. (16) in problem (RLX), the above lemma can be easily proved by analyzing sensor's energy profiles at each

location, which only relates to the duration spent at sojourn/virtual points. We omit the proof here to conserve space. □

Lemma 5 *Suppose P^* is an optimal solution of problem (RLX), which consists of $\varepsilon_{il}^*, U^*(x_l), \mu_{il}^*, U^*(\nu_l), \eta_i^*, H_i^*, \tau_i^*, T_0^*$ and the maximum network lifetime*

$$T^* = \sum_{l\in N}[U^*(x_l) + U^*(\nu_l)].$$

We can always construct a solution of problem (LP-T) with the network lifetime $T' \geq T^*$.

Proof Based on Lemma 4, we can regulate the charger's travel path to a single TSP path ($L = N$), and then problem (RLX) can be solved by CPLEX. The resulted solution is denoted by P^*.

Next, we construct a solution $\overline{P}$ as follows: we keep the charger's travel path, sojourn and travel durations unchanged while data routing is altered to the minimum energy routing. Specifically, $\overline{P}$ consists of $\varepsilon_{il}, U^*(x_l), \mu_{il}, U^*(\nu_l), \eta_i, H_i, \tau_i, T_0$ and $\overline{T}$ (note that $\overline{T} = T^*$). Suppose the total energy consumption of solution P^* and $\overline{P}$ during the operational interval are ω^* and ω, respectively. To prove Lemma 5, we need to prove: (i) $\omega^* \geq \omega$; (ii) $T_0^* \geq T_0$; (iii) For P^*, Eq. (10) reaches equality.

(i) Based on the definition of ω^* and ω, we have:

$$\omega^* = \sum_{i\in N}\sum_{l\in N} e_{il}^* \quad \text{and} \quad \omega = \sum_{i\in N}\sum_{l\in N} e_{il}$$

where

$$e_{il}^* = (\varepsilon_{il}^* + \mu_{il}^*\lambda_l)U^*(x_l) + [U^*(\nu_l) - \lambda_l U^*(x_l)]\eta_i^*$$

and

$$e_{il} = (\varepsilon_{il} + \mu_{il}\lambda_l)U^*(x_l) + [U^*(\nu_l) - \lambda_l U^*(x_l)]\eta_i$$

Solution $\overline{P}$ adopts the minimum energy routing during the whole network lifetime. Therefore, for any $l \in L$, we have $\sum_{i\in N}\varepsilon_{il} \leq \sum_{i\in N}\varepsilon_{il}^*$, $\sum_{i\in N}\mu_{il} \leq \sum_{i\in N}\mu_{il}^*$ and $\sum_{i\in N}\eta_i \leq \sum_{i\in N}\eta_i^*$. Thus, we have

$$\begin{aligned}\omega^* - \omega = \sum_{l\in N}\Bigg\{&\left(\sum_{i\in N}\varepsilon_{il}^* - \sum_{i\in N}\varepsilon_{il}\right)U^*(x_l)\\ &+\left(\sum_{i\in N}\mu_{il}^* - \sum_{i\in N}\mu_{il}\right)\lambda_l U^*(x_l)\\ &+\left(\sum_{i\in N}\eta_i^* - \sum_{i\in N}\eta_i\right)[U^*(\nu_l) - \lambda_l U^*(x_l)]\Bigg\} \geq 0\end{aligned}$$

(ii) Based on energy conservation, we have:

$$\omega^* + Ne_0T_0^* = Nh_0 + \varpi_0\sum_{i\in N}\tau_i^* + \varpi\sum_{i\in N}U^*(x_i) \quad (25)$$

and

$$\omega + Ne_0T_0 = Nh_0 + \varpi_0\sum_{i\in N}\tau_i + \varpi\sum_{i\in N}U^*(x_i) \quad (26)$$

Let Eq. (25) minus Eq. (26), then we can obtain

$$(\varpi_0 - Ne_0)\left(\sum_{i\in N}\tau_i^* - \sum_{i\in N}\tau_i\right) = \omega^* - \omega \geq 0$$

The charging rate during the initial time ϖ_0 is larger than the total energy consumption rate, i.e., $\varpi_0 - Ne_0 > 0$ holds (otherwise, sensor batteries may deplete before the beginning of the operational interval T_0). Thus we obtain $\sum_{i\in N}\tau_i^* \geq \sum_{i\in N}\tau_i$. Based on $T_0 = t_{TL} + \sum_{i\in N}\tau_i$, we can derive $T_0^* \geq T_0$.

(iii) This can be explained intuitively. Suppose the equality is not reached, which means that part of the total energy E is unallocated. Then, we can always find a method to reallocate the unallocated energy and obtain a larger T, which contradicts the fact that T^* is the maximum network lifetime. Thus we have:

$$Nh_0 + \varpi_0\sum_{i\in N}\tau_i^* + \varpi\sum_{l\in N}U^*(x_l) = E$$

The above equation is based on the fact that we are in full charge of energy allocation of the sensor network. To prove Lemma 5, we first need to prove that $\overline{P}$ is a feasible solution of problem (LP-T). Since H_i is an intermediate parameter that can be removed by reformulation and $U^*(\nu_l) \geq \lambda_l U^*(x_l)$ holds, we only need to prove that Eq. (10) is satisfied by $\overline{P}$. Based on (i) and (ii), we can derive:

$$\begin{aligned}&Nh_0 + \varpi_0\sum_{i\in N}\tau_i + \varpi\sum_{l\in N}U^*(x_l) = \omega + Ne_0T_0\\ &\leq \omega^* + Ne_0T_0^* = Nh_0 + \varpi_0\sum_{i\in N}\tau_i^* + \varpi\sum_{l\in N}U^*(x_l) = E\end{aligned}$$

Thus $\overline{P}$ is feasible to problem (LP-T). The above equation also shows that a part of energy is unallocated in solution $\overline{P}$. Based on (iii), we can always construct a solution of problem (LP-T) with longer network lifetime $T' \geq \overline{T} = T^*$, which concludes the proof. □

Finally, we prove Theorem 3.

Proof Suppose P^* is an optimal solution of problem (RLX) with the maximum network lifetime T^*. Based on Lemma 5, we can always construct a solution of problem (LP-T), e.g., $\overline{P}$, with a network lifetime $\overline{T} \geq T^*$. Meanwhile, based on

Lemma 3, solution $\overline{P}$ is also feasible to problem (RLX). And the maximum network lifetime of problem (RLX) is T^*. Hence, solution $\overline{P}$ is also the optimal solution of problem (RLX) with the network lifetime $\overline{T} = T^*$, which concludes the proof. □

Proof of Theorem 4

Proof As to $W = 1$, problem (LP-W) equals to problem (LP-T). Here, we emphasize on the $W > 1$ situation. Let $U^w(x_l) = WU(x_l)$ and $U^w(v_l) = WU(v_l)$, then the objective function of problem (LP-W) becomes

$$T = \sum_{l \in N} [U^w(x_l) + U^w(v_l)] \tag{27}$$

And constraint Eq. (19) is converted to:

$$\sum_{l \in N} e_{il}^w - \varpi U^w(x_i) = H_i \tag{28}$$

where

$$e_{il}^w = \varepsilon_{il} U^w(x_l) + \mu_{il} \lambda_l U^w(x_l) + (U^w(v_l) - \lambda_l U^w(x_l))\eta_i$$

Similarly, constraint Eq. (20) is converted to:

$$Nh_0 + \varpi_0 \sum_{i \in N} \tau_i + \varpi \sum_{l \in N} U^w(x_l) \leq E \tag{29}$$

Then, based on the new objective function Eq. (27) and constraints Eqs. (28), (29), problem (LP-W) can be equivalently transformed to problem (LP-T), which concludes the proof. □

References

Anastasi, G., Conti, M., Monaldi, E., Passarella, A.: An adaptive data-transfer protocol for sensor networks with data mules. In: 2007 International Symposium on a World of Wireless, Mobile and Multimedia Networks (WoWMoM 2007), 18–21 June 2007, Helsinki, Finland, Proceedings, pp. 1–8. IEEE Computer Society (2007). https://doi.org/10.1109/WOWMOM.2007.4351776

Chen, L., Liu, S., Zhou, Y.C., Cui, T.J.: An optimizable circuit structure for high-efficiency wireless power transfer. IEEE Trans. Ind. Elect. **60**(1), 339–349 (2013). https://doi.org/10.1109/TIE.2011.2179275

Dai, H., Liu, Y., Chen, G., Wu, X., He, T.: Safe charging for wireless power transfer. In: 2014 IEEE Conference on Computer Communications, INFOCOM 2014, Toronto, Canada, April 27–May 2, 2014, pp. 1105–1113. IEEE (2014). https://doi.org/10.1109/INFOCOM.2014.6848041

Fu, L., Cheng, P., Gu, Y., Chen, J., He, T.: Minimizing charging delay in wireless rechargeable sensor networks. In: Proceedings of the IEEE INFOCOM 2013, Turin, Italy, April 14–19, 2013, pp. 2922–2930. IEEE (2013). https://doi.org/10.1109/INFCOM.2013.6567103

Guo, S., Wang, C., Yang, Y.: Mobile data gathering with wireless energy replenishment in rechargeable sensor networks. In: Proceedings of the IEEE INFOCOM 2013, Turin, Italy, April 14–19, 2013, pp. 1932–1940. IEEE (2013). https://doi.org/10.1109/INFCOM.2013.6566993

He, S., Chen, J., Jiang, F., Yau, D.K.Y., Xing, G., Sun, Y.: Energy provisioning in wireless rechargeable sensor networks. IEEE Trans. Mob. Comput. **12**(10), 1931–1942 (2013). https://doi.org/10.1109/TMC.2012.161

IBM ILOG CPLEX Optimizer (2016). http://www-01.ibm.com/software/integration/optimization/cplex-optimizer/

Kellogg, B., Parks, A.N., Gollakota, S., Smith, J.R., Wetherall, D.: Wi-fi backscatter: internet connectivity for rf-powered devices. In: Bustamante, F.E., Hu, Y.C., Krishnamurthy, A., Ratnasamy, S. (eds.) ACM SIGCOMM 2014 Conference, SIGCOMM'14, Chicago, IL, USA, August 17–22, 2014, pp. 607–618. ACM (2014). https://doi.org/10.1145/2619239.2626319

Kurs, A., Karalis, A., Moffatt, R., Joannopoulos, J.D., Fisher, P., Soljacic, M.: Wireless power transfer via strongly coupled magnetic resonances. Science **317**(5834), 83–86 (2007)

Lee, S.H., Lorenz, R.D.: Development and validation of model for 95%-efficiency 220-w wireless power transfer over a 30-cm air gap. IEEE Trans. Ind. Appl. **47**(6), 2495–2504 (2011)

Li, Z., Liu, Y., Li, M., Wang, J., Cao, Z.: Exploiting ubiquitous data collection for mobile users in wireless sensor networks. IEEE Trans. Parallel Distrib. Syst. **24**(2), 312–326 (2013). https://doi.org/10.1109/TPDS.2012.92

Liu, V., Parks, A.N., Talla, V., Gollakota, S., Wetherall, D., Smith, J.R.: Ambient backscatter: wireless communication out of thin air. In: Chiu, D.M., Wang, J., Barford, P., Seshan, S. (eds.) ACM SIGCOMM 2013 Conference, SIGCOMM'13, Hong Kong, China, August 12–16, 2013, pp. 39–50. ACM (2013). https://doi.org/10.1145/2486001.2486015

Naderi, M.Y., Chowdhury, K.R., Basagni, S., Heinzelman, W.B., De, S., Jana, S.: Experimental study of concurrent data and wireless energy transfer for sensor networks. In: IEEE Global Communications Conference, GLOBECOM 2014, Austin, TX, USA, December 8–12, 2014, pp. 2543–2549. IEEE (2014). https://doi.org/10.1109/GLOCOM.2014.7037190

Naderi, M.Y., Chowdhury, K.R., Basagni, S., Heinzelman, W.B., De, S., Jana, S.: Surviving wireless energy interference in rf-harvesting sensor networks: An empirical study. In: Eleventh Annual IEEE International Conference on Sensing, Communication, and Networking Workshops, SECON Workshops 2014 Singapore, June 30–July 3, 2014, pp. 39–44. IEEE (2014). https://doi.org/10.1109/SECONW.2014.6979703

Park, U., Heidemann, J.S.: Data muling with mobile phones for sensornets. In: J. Liu, P. Levis, K. Römer (eds.) Proceedings of the 9th International Conference on Embedded Networked Sensor Systems, SenSys 2011, Seattle, WA, USA, November 1–4, 2011, pp. 162–175. ACM (2011). https://doi.org/10.1145/2070942.2070960

Peng, Y., Li, Z., Zhang, W., Qiao, D.: Prolonging sensor network lifetime through wireless charging. In:Proceedings of the 31st IEEE Real-Time Systems Symposium, RTSS 2010, San Diego, California, USA,November 30–December 3, 2010, pp. 129–139. IEEE Computer Society (2010). https://doi.org/10.1109/RTSS.2010.35

Powercast (2017). http://www.powercastco.com

Qu, Y., Xu, K., Liu, J., Chen, W.: Towards a practical energy conservation mechanism with assistance of resourceful mules. IEEE Internet Things J. **2**(2), 145–158 (2015)

Shi, Y., Hou, Y.T.: Some fundamental results on base station movement problem for wireless sensor networks. IEEE/ACM Trans. Netw. **20**(4), 1054–1067 (2012). https://doi.org/10.1109/TNET.2011.2171990

Shi, Y., Xie, L., Hou, Y.T., Sherali, H.D.: On renewable sensor networks with wireless energy transfer. In INFOCOM 2011. 30th IEEE International Conference on Computer Communications, Joint Conference of the IEEE Computer and Communications Societies, 10–15 April 2011, Shanghai, China, pp. 1350–1358. IEEE (2011). https://doi.org/10.1109/INFCOM.2011.5934919

Somasundara, A.A., Kansal, A., Jea, D.D., Estrin, D., Srivastava, M.B.: Controllably mobile infrastructure for low energy embedded networks. IEEE Trans. Mob. Comput. **5**(8), 958–973 (2006). https://doi.org/10.1109/TMC.2006.109

Xie, L., Shi, Y., Hou, Y.T., Lou, A.: Wireless power transfer and applications to sensor networks. IEEE Wirel. Commun. Mag. **20**(4), (2013). https://doi.org/10.1109/MWC.2013.6590061

Xie, L., Shi, Y., Hou, Y.T., Lou, W., Sherali, H.D., Midkiff, S.F.: Bundling mobile base station and wireless energy transfer: Modeling and optimization. In: Proceedings of the IEEE INFOCOM 2013, Turin, Italy, April 14–19, 2013, pp. 1636–1644. IEEE (2013). https://doi.org/10.1109/INFCOM.2013.6566960

Yigitel, M.A., Incel, O.D., Ersoy, C.: QoS-aware MAC protocols for wireless sensor networks: A survey. Elsevier Comput. Netw. **55**(8), 1982–2004 (2011). https://doi.org/10.1016/j.comnet.2011.02.007

Zhang, S., Qian, Z., Kong, F., Wu, J., Lu, S.: P^3: Joint optimization of charger placement and power allocation for wireless power transfer. In: 2015 IEEE Conference on Computer Communications, INFOCOM 2015, Kowloon, Hong Kong, April 26 May 1, 2015, pp. 2344–2352. IEEE (2015). https://doi.org/10.1109/INFOCOM.2015.7218622

Zhu, T., Gu, Y., He, T., Zhang, Z.: eshare: a capacitor- driven energy storage and sharing network for long-term operation. In: J. Beutel, D. Ganesan, J.A. Stankovic (eds.) Proceedings of the 8th International Conferenceon Embedded Networked Sensor Systems, SenSys 2010, Zurich, Switzerland, November 3–5, 2010, pp. 239–252. ACM (2010). https://doi.org/10.1145/1869983.1870007

Qi Tan received the BEng degree in 2012. Currently he is a master student in the Department of Computer Science & Technology of Tsinghua University, Beijing, China. His research interests include network architecture and wireless sensor network.

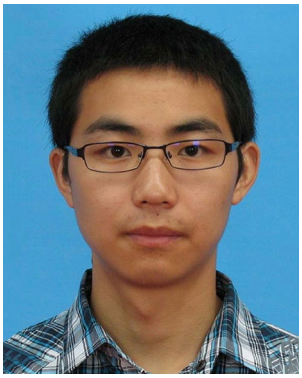

Yi Qu received the BEng degree in software engineering from University of Electronic Science and Technology of China in 2011. Currently he is a Ph.D. student in the Department of Computer Science & Technology of Tsinghua University, Beijing, China. His research interests include wireless network and wireless sensor network.

Ke Xu received his Ph.D. from the Department of Computer Science & Technology of Tsinghua University, Beijing, China, where he serves as a full professor. He has published more than 100 technical papers and holds 20 patents in the research areas of next generation Internet, P2P systems, Internet of Things (IoT), network virtualization and optimization. As a member of ACM and an associate editor of Springer journal Networking Science, he has guest edited several special issues in IEEE and Springer Journals. He is serving as an associate editor of Springer journal Networking Science. He is also holding visiting professor position of University of Essex.

Haiyang Wang received the PhD degree in computing science from Simon Fraser University, Burnaby, BC, Canada, in 2013. He is currently an assistant professor at the Department of Computer Science, University of Minnesota Duluth, MN. His research interests include cloud computing, big data, socialized content sharing, multimedia communications, and peer-to-peer networks. He is a member of the IEEE.

Dan Wang received the BSc degree from Peking University, Beijing, the MSc degree from Case Western Reserve University, Cleveland, OH, and the PhD degree from Simon Fraser University, Vancouver, Canada, all in computer science. He is an associate professor at the Department of Computing, The Hong Kong Polytechnic University, Hung Hom, Kowloon, Hong Kong. His research interest includes sensor networks, internet routing, and applications. He is a senior member of the IEEE.

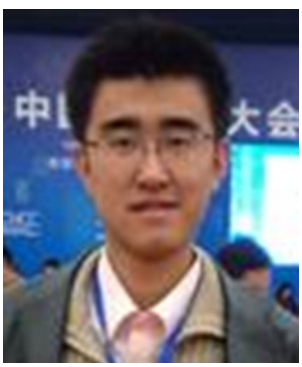

Meng Shen received the B.Eng degree from Shandong University, Jinan, China in 2009, and the Ph.D degree from Tsinghua University, Beijing, China in 2014, both in computer science. Currently he serves in Beijing Institute of Technology, Beijing, China, as an assistant professor. His research interests include traffic engineering and network security.He is a member of the IEEE.